J|A|C|S
ARTICLES
Published on Web 01/24/2006

Kinetics and Mechanism of Methane, Methanol, and Dimethyl Ether C−H Activation with Electrophilic Platinum Complexes

Jonathan S. Owen, Jay A. Labinger,* and John E. Bercaw*

Contribution from the Arnold and Mabel Beckman Laboratories of Chemical Synthesis, California Institute of Technology, Pasadena, California 91125

Received September 16, 2005; E-mail: jal@its.caltech.edu

Abstract: The relative rates of C−H activation of methane, methanol, and dimethyl ether by [(N-N)PtMe(TFE-d_3)]$^+$ ((N-N) = ArN═C(Me)−C(Me)═NAr; Ar = 3,5-di-*tert*-butylphenyl, TFE-d_3 = CF_3CD_2OD) (**2(TFE)**) were determined. Methane activation kinetics were conducted by reacting **2(TFE)-^{13}C** with 300−1000 psi of methane in single-crystal sapphire NMR tubes; clean second-order behavior was obtained ($k = 1.6 \pm 0.4 \times 10^{-3}$ M^{-1} s^{-1} at 330 K; $k = 2.7 \pm 0.2 \times 10^{-4}$ M^{-1} s^{-1} at 313 K). Addition of methanol to solutions of **2(TFE)** rapidly establishes equilibrium between methanol (**2(MeOD)**) and trifluoroethanol (**2(TFE)**) adducts, with methanol binding preferentially ($K_{eq} = 0.0042 \pm 0.0006$). C−H activation gives [(N-N)Pt(CH_2OD)(MeOD)]$^+$ (**4**), which is unstable and reacts with [(RO)B(C_6F_5)$_3$]$^-$ to generate a pentafluorophenyl platinum complex. Analysis of kinetics data for reaction of **2** with methanol yields $k = 2.0 \pm 0.2 \times 10^{-3}$ M^{-1} s^{-1} at 330 K, with a small kinetic isotope effect ($k_H/k_D = 1.4 \pm 0.1$). Reaction of dimethyl ether with **2(TFE)** proceeds similarly ($K_{eq} = 0.023 \pm 0.002$, 313 K; $k = 5.5 \pm 0.5 \times 10^{-4}$ M^{-1} s^{-1}, $k_H/k_D = 1.5 \pm 0.1$); the product obtained is a novel bis(alkylidene)-bridged platinum dimer, [(diimine)Pt(μ-CH_2)(μ-(CH(OCH_3))Pt(diimine)]$^{2+}$ (**5**). Displacement of TFE by a C−H bond appears to be the rate-determining step for all three substrates; comparison of the second-order rate constants ($k_{(methane)}/k_{(methanol)} = 1/1.3$, 330 K; $k_{(methane)}/k_{(dimethyl\ ether)} = 1/2.0$, 313 K) shows that this step is relatively unselective for the C−H bonds of methane, methanol, or dimethyl ether. This low selectivity agrees with previous estimates for oxidations with aqueous tetrachloroplatinate(II)/hexachloroplatinate(IV), suggesting a similar rate-determining step for those reactions.

Introduction

The rising cost of oil and the fear of high carbon dioxide levels in the atmosphere are leading scientists to search for cheap alternatives to coal and oil.[1] The direct aerobic oxidation of methane to useful chemicals is one potential approach to this problem. Unfortunately, such processes are complicated by the increasing reactivity of its oxidation products. Most oxidants capable of reacting with methane (BDE(C−H) = 104 kcal/mol) follow a hydrogen atom abstraction route and hence react more readily with the weaker C−H bonds of methanol (BDE(C−H) = 93 kcal/mol), placing an inherent limit on the yield.[2] Nonetheless, a few oxidation catalysts based on platinum(II), palladium(II), and mercury(II) salts have been shown to produce high yields of partially oxidized products.[3] In fuming sulfuric acid, a platinum complex was shown to catalyze the oxidation of methane to methyl bisulfate in up to 70% yield.[3c] Under these conditions, it was estimated that methane can be as much as 100 times more reactive than methyl bisulfate, its oxidation product.[2c] Studies on the aqueous chloroplatinate system pioneered by Shilov suggest that methyl groups (or methane) and hydroxymethyl groups (or methanol) exhibit similar reactivity, with estimated relative rate constants ranging from 1.5:1 to 1:5.[4] The origin of these unusual oxidation selectivities is not clear.

Several groups have studied the thermodynamic and kinetic selectivity of C−H bond activation by organometallic transition metal complexes.[5] In general, the regioselectivity of such C−H activations is opposite to that of hydrogen atom abstraction reactions, with stronger bonds being more reactive, leading to the following selectivity order: H−C(sp^2) > 1° H−C(sp^3) > 2° H−C(sp^3) > 3° H−C(sp^3). Most studies have been limited to alkanes and arenes because the metal complexes suited to mechanistic studies have limited functional group tolerance. Little is known about the influence of heteroatom substitution on the rate of C−H bond activation.[6]

Mechanistic interpretation of this selectivity is complicated by the fact that C−H activation is a multistep and, often,

(1) Arakawa, H. et al. *Chem. Rev.* **2001**, *101*, 953−996.
(2) (a) Labinger, J. A. *Catal. Let.* **1988**, *1*, 371−375. (b) Crabtree, R. H. *Chem. Rev.* **1995**, *95*, 987−1007. (c) Labinger, J. A.; Bercaw, J. E.; Luinstra, G. A.; Lyon, D. K.; Herring, A. M. In *Natural Gas Conversion II*; Proceedings of the Third International Gas Conversion Symposium, Sydney, Australia, July 4−9, 1993; Howe, R. F., Curry-Hyde, E., Eds.; Elsevier: Amsterdam, 1994; pp 515−520.
(3) (a) Stahl, S. S.; Labinger, J. A.; Bercaw, J. E. *Angew. Chem., Int. Ed.* **1998**, *37*, 2180−2192 and references therein. (b) Periana, R. A.; Taube, D. J.; Evitt, E. R.; Loffler, D. G.; Wentrcek, P. R.; Voss, G.; Masuda, T. *Science* **1993**, *259*, 340−343. (c) Periana, R. A.; Taube, D. J.; Gamble, S.; Taube, H.; Satoh, T.; Fujii, H. *Science* **1998**, *280*, 560−564.
(4) (a) Labinger, J. A.; Herring, A. M.; Bercaw, J. E. *J. Am. Chem. Soc.* **1990**, *112*, 5628−5629. (b) Labinger, J. A.; Herring, A. M.; Lyon, D. K.; Luinstra, G. A.; Bercaw, J. E.; Horvath, I. T.; Eller, K. *Organometallics* **1993**, *12*, 895−905. (c) Sen, A.; Benvenuto, M. A.; Lin, M. R.; Hutson, A. C.; Basickes, N. *J. Am. Chem. Soc.* **1994**, *116*, 998−1003. These estimates are complicated by the ubiquitous formation of metallic Pt, which is a good alcohol oxidation catalyst.
(5) Arndtsen, B. A.; Bergman, R. O.; Mobley, T. A.; Peterson, T. H. *Acc. Chem. Res.* **1995**, *28*, 154−162 and references therein.

Scheme 1

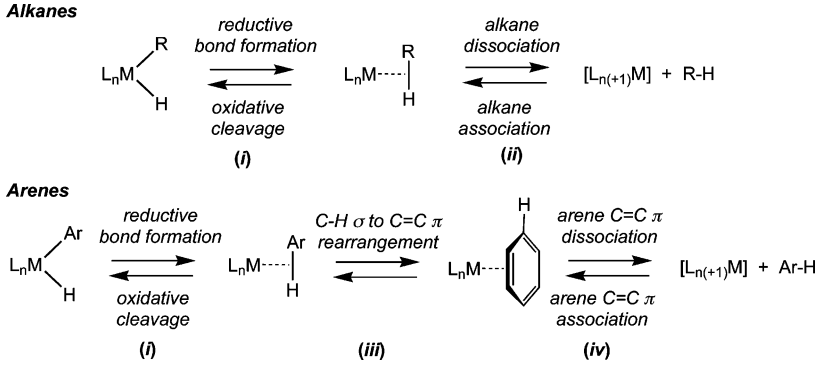

reversible reaction.[7] In particular, the formation of arene C═C π-complexes and C−H σ-complexes complicates direct studies of the C−H bond cleavage and forming steps. Most often this is revealed in studies on the microscopic reverse of C−H bond oxidative addition (Scheme 1). For systems where reductive elimination of alkane or arene is highly endothermic, C−H bond formation is typically a fast and reversible first (step ***i***) followed by rate-determining loss of hydrocarbon (step ***ii*** or ***iv***). The *inverse* kinetic isotope effects commonly observed in these reactions are believed to result from the product of an inverse equilibrium isotope effect for (***i***) and a small, normal kinetic isotope effect for alkane decoordination (***ii***).[8] Several examples of direct spectroscopic and kinetic evidence for the intermediacy of arene complexes in arene C−H bond activation have been reported,[7e] but only a few studies of *alkane* activation provide kinetic information on individual microscopic steps.[9,10]

We have previously exploited diimine-ligated platinum(II) and palladium(II) alkyl complexes as model systems in extensive mechanistic studies of C−H activation for arenes and alkyl-substituted arenes.[11] Here we use the Pt(II) model to investigate the relative rates and mechanism of C−H activation for methane, methanol, and dimethyl ether. In addition, spectroscopic and crystallographic characterization of the primary and/or secondary products of methanol and dimethyl ether C−H activation are described.

Scheme 2

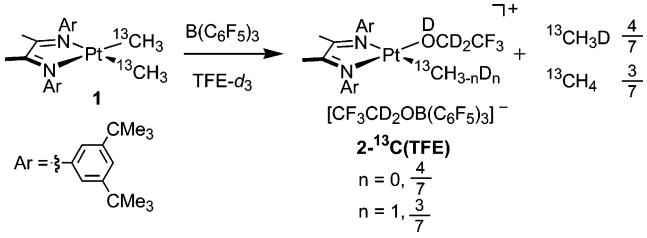

Scheme 3

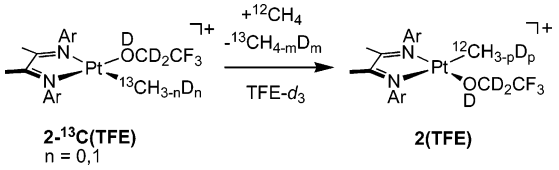

Results

Reaction of Methane with [(N-N)Pt($^{13}CH_{3-n}D_n$)(DOCD$_2$CF$_3$)]$^+$[CF$_3$CD$_2$OB(C$_6$F$_5$)$_3$]$^-$ (2-^{13}C(TFE)). To study the kinetics of methane activation, (diimine)platinumdimethyl complex **1-^{13}C** was prepared from the diimine ligand ArN═C(Me)−C(Me)═NAr (Ar = 3,5-di-*tert*-butylphenyl) and [(μ-SMe$_2$)Pt($^{13}CH_3$)$_2$]$_2$. Protonolysis of **1-^{13}C** with tris(pentafluorophenyl)borane (B(C$_6$F$_5$)$_3$) in anhydrous CF$_3$CD$_2$OD (TFE-d_3) produces **2-^{13}C(TFE)**, trifluoroethoxytris(pentafluorophenyl)borate, and methane. Although only 1 equiv of B(C$_6$F$_5$)$_3$ is required by stoichiometry, 2 equiv is generally needed to achieve clean formation of **2**; the reason is not known. Both **2-^{13}C(TFE)** and methane are obtained as a statistical mixture of isotopologs (Scheme 2), as previously reported.[11d]

Upon pressurizing solutions of **2-^{13}C(TFE)** in single-crystal sapphire NMR tubes with dry methane-^{12}C, formation of **2-^{12}C(TFE)** is observed in the ^{1}H NMR spectrum (Scheme 3). Disappearance of the ^{1}H NMR signal for **2-^{13}C(TFE)** and appearance of that for **2-^{12}C(TFE)** occur at similar rates. Data for kinetics were obtained by monitoring the ^{13}C NMR signal for **2-^{13}C(TFE)** over time, at 330 and 313 K, in the presence of 300−1000 psi of added methane. The data were analyzed as a function of the concentration of dissolved methane (measured by NMR). The first-order decay of the ^{13}C signal exhibits a linear dependence on [methane] at both 330 K ($k_2 = 1.6 \pm 0.4 \times 10^{-3}$ M^{-1} s^{-1}) and 313 K ($k_2 = 2.7 \pm 0.2 \times 10^{-4}$ M^{-1} s^{-1}) (Table 1 and Figure 1).

Methane activation is accompanied by a much slower decomposition reaction, indicated by appearance of new NMR

(6) See, for example: (a) Vetter, A. J.; Jones, W. D. *Polyhedron* **2004**, *23*, 413−417. (b) Lawrence, J. D.; Takahashi, M.; Bae, C.; Hartwig, J. F. *J. Am. Chem. Soc.* **2004**, *126*, 15334−15335.
(7) (a) Crabtree, R. H. *Chem. Rev.* **1985**, *85*, 245−269. (b) Crabtree, R. H. *Chem. Rev.* **1995**, *95*, 987−1007. (c) Hall, C.; Perutz, R. N. *Chem. Rev.* **1996**, *96*, 3125−3146. (d) Shilov, A. E.; Shul'pin, G. B. *Chem. Rev.* **1997**, *97*, 2879−2932. (e) Fekl, U.; Goldberg, K. I. *Adv. Inorg. Chem.* **2003**, *54*, 259−320. (f) Lersch, M.; Tilset, M. *Chem. Rev.* **2005**, *105*, 2471−2526.
(8) Jones, W. D. *Acc. Chem. Res.* **2003**, *36*, 140−146.
(9) (a) Schaller, C. P.; Bonanno, J. B.; Wolczanski, P. T. *J. Am. Chem. Soc.* **1994**, *116*, 4133−4134. (b) Bennett, J. L.; Wolczanski, P. T. *J. Am. Chem. Soc.* **1997**, *119*, 10696−10719. (c) Northcutt, T. O.; Wick, D. G.; Vetter, A. J.; Jones, W. D. *J. Am. Chem. Soc.* **2001**, *123*, 7357−7270. (d) Vetter, A. J.; Flaschenriem, C.; Jones, W. D. *J. Am. Chem. Soc.* **2005**, *127*, 12315−12322.
(10) (a) Weiller, B. H.; Wasserman, E. P.; Bergman, R. G.; Moore, C. B.; Pimentel, G. C. *J. Am. Chem. Soc.* **1989**, *111*, 8288. (b) Bengali, A. A.; Schultz, R. H.; Moore, C. B.; Bergman, R. G. *J. Am. Chem. Soc.* **1994**, *116*, 9585−9589. (c) Schultz, R. H.; Bengali, A. A.; Tauber, M. J.; Weiller, B. H.; Wasserman, E. P.; Kyle, K. R.; Moore, C. B.; Bergman, R. G. *J. Am. Chem. Soc.* **1994**, *116*, 7369−7377.
(11) (a) Zhong, A. H.; Labinger, J. A.; Bercaw, J. E. *J. Am. Chem. Soc.* **2002**, *124*, 1378−1399. (b) Johansson, L.; Tilset, M.; Labinger, J. A.; Bercaw, J. E. *J. Am. Chem. Soc.* **2002**, *122*, 10846−10855. (c) Ackerman, L. J.; Sadighi, J. P.; Kurtz, D. M.; Labinger, J. A.; Bercaw, J. E. *Organometallics* **2003**, *22*, 3884−3890. (d) Heyduk, A. F.; Driver, T. G.; Labinger, J. A.; Bercaw, J. E. *J. Am. Chem. Soc.* **2004**, *126*, 15034−15035. (e) Driver, T. G.; Day, M. W.; Labinger, J. A.; Bercaw, J. E. *Organometallics* **2005**, *24*, 3644−3654.

Table 1. Methane Activation Kinetics with **2**

temp (K)	[Pt] (M)	methane (psi)	$[CH_4]$ (M)	k_{obs} (s^{-1})	k_2[a] ($M^{-1}\,s^{-1}$)
313	0.0145	570	0.393	0.000059	0.000266
313	0.0145	835	0.690	0.000101	0.000275
313	0.0145	1020	0.855	0.000121	0.000266
330	0.00944	300	0.298	0.000288	0.00181
330	0.00944	400	0.370	0.000283	0.00143
330	0.0145	500	0.423	0.000350	0.00157
330	0.0218	503	0.510	0.000376	0.00140
330	0.0145	550	0.488	0.000385	0.00150
330	0.0145	700	0.617	0.000540	0.00169

[a] Calculated from $\{k_2 = (k_{obs} - k_i)/[CH_4] \times 2\}$, where k_i is taken from the intercept of k_{obs} versus [methane], and the factor of 2 is included for the equal rates of the forward and back reaction. See text for discussion.

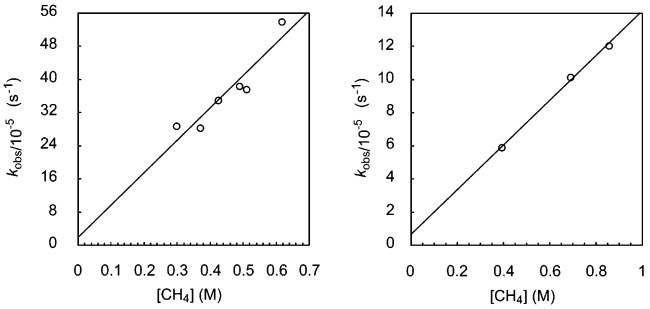

Figure 1. Plots of k_{obs} versus [methane] at 330 K (left) and 313 K (right).

Scheme 4

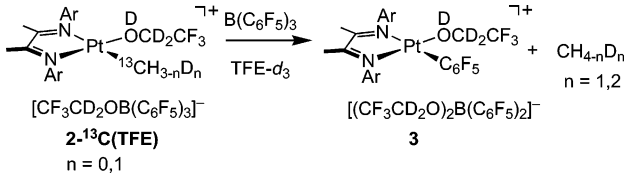

signals as well as the nonzero intercept in Figure 1 ($k_{decomp} = 1.8 \times 10^{-5}$ s^{-1}, 330 K; $k_{decomp} = 6.8 \times 10^{-6}$ s^{-1}, 313 K). In the absence of added substrate, **2** decomposes to give the same species (along with CH_3D and CH_2D_2) at an initial first-order rate similar to the intercept value ([**2(TFE)**] = 15.2 mM, $[B(C_6F_5)_3]$ = 30.3 mM, $k_{obs} = 4 \times 10^{-5}$ s^{-1}, 330 K). The decomposition product was identified as a pentafluorophenyl platinum complex (**3**) (Scheme 4) by the close similarity of NMR parameters to those of a previously reported analogue.[11e] In further confirmation of the assignment, electrospray mass spectra of these samples diluted with methanol show a large peak at *m/z* = 854.3 amu, consistent with a methanol-bound pentafluorophenyl platinum cation (**3(MeOD)**), and solutions of **2** left exposed to air produce crystals of the hydroxytris(pentafluorophenyl)borate pentafluorophenyl complex **3(HOB(C_6F_5)$_3$)**, differing from the previous analogue[11e] only by the substituents on the diimine ligands, as established crystallographically.[12] Exposure of the sample to moisture most likely generates a water adduct with the Lewis acidic borane, and the anion ($[B(C_6F_5)_3OH]^-$) binds to the metal center, generating an insoluble charge-neutral complex.

Reaction of Methanol with 2. On addition of anhydrous methanol-d_1 to solutions of **2(TFE)**, a new set of NMR signals appears, indicative of a rapid equilibrium between methanol-bound (**2(MeOD)**) and trifluoroethanol-bound (**2(TFE)**) platinum cations, with the former strongly favored ($K_{eq} = 0.0042 \pm 0.0006$, 330 K). Additional broad signals for methanol bound to tris(pentafluorophenyl)borane are visible in the ^1H and ^{13}C NMR spectra; their shape and shift depend on the probe temperature and the concentration of added methanol. Over several hours, ^1H NMR spectroscopy shows formation of methane isotopologs, a set of ligand resonances for a new platinum complex, and additional resonances in the region typical of methanol C−H bonds. These new resonances subsequently disappear, with the concomitant appearance of signals characteristic of methanol-bound pentafluorophenyl platinum cation (**3(MeOD)**). The pentafluorophenyl complex appears in these reactions at a rate considerably faster than that in methane activation (see above); in reactions carried out with a high concentration of methanol, **3** is the major (>90%) observable product.

The methane generated in these reactions is a mixture of not only CH_4 and CH_3D (as expected for C−H activation of methanol-d_1 by **2(TFE)**, which contains approximately equal amounts of Pt−CH_3 and Pt−CH_2D) but also CH_2D_2. The relative amount of CH_2D_2 decreases with increasing concentration of methanol-d_1; for [methanol-d_1] = 0.123 M, CH_4:CH_2D_2 ≈ 1:2, whereas for [methanol-d_1] = 1.23 M, CH_4:CH_2D_2 ≈ 5:1. Reactions in which CD_3OD is substituted for CH_3OD produce primarily CH_3D and CH_2D_2 with essentially no CH_4.

Concentrations of the initially formed platinum complex sufficient for characterization by NMR spectroscopy may be obtained by using relatively low concentrations of added methanol. Reaction of **2** with 3 equiv of $^{13}CH_3OH$ produces a new ^{13}C NMR signal at $\delta = -4$ ppm with broad ^{195}Pt satellites (J = 732 Hz). In the ^1H-coupled ^{13}C NMR spectrum, this resonance appears as a 1:2:1 triplet (J = 134 Hz), consistent with a platinum-bound sp^3-hybridized CH_2X fragment. $^1H-\{^{13}C\}$ Heteronuclear Multiple Quantum Coherence (HMQC) spectroscopy is useful for identifying signals resulting from protons directly attached to ^{13}C atoms. The 1D HMQC spectrum of the product obtained from **2(TFE)** and $^{13}CH_3OH$ (present as mostly $^{13}CH_3OD$ in CF_3CD_2OD solvent) shows four signals, derived from the labeled methanol, that are greatly enhanced relative to the signals for the diimine ligand (Figure 2). In addition to the signals for bound methanol in unreacted **2($^{13}CH_3OD$)** (δ = 2.94 ppm) and decomposition product **3($^{13}CH_3OD$)** (δ = 2.90 ppm), two new signals are observed at δ = 2.62 and 2.72 ppm, with an intensity ratio of 3:2. The 2D HMQC spectrum (Figure 3) shows how these ^1H resonances correlate with the ^{13}C signals for the carbons to which they are bound. The signal at δ = 2.72 ppm correlates with the high-field ^{13}C resonance noted above ($\delta = -4$ ppm), while the signal at δ = 2.62 ppm correlates with a ^{13}C resonance at δ = 55.8 ppm, close to the O-bound methanol signals of **2($^{13}CH_3OD$)** (δ = 57.1 ppm) and **3($^{13}CH_3OD$)** (δ = 56.2 ppm). On the basis of these data, we formulate the intermediate as the hydroxymethyl complex ($[(N\text{-}N)Pt(CH_2OD)(DOCH_3)]^+$) (**4**, Scheme 5).[13]

Kinetics of Methanol Activation. Reactions of **2** with varying concentrations of CH_3OD or CD_3OD at 330 K were

(12) Crystallographic data have been deposited at the CCDC, 12 Union Road, Cambridge CB2 1EZ, UK and copies can be obtained on request, free of charge, by quoting the publication citation and the deposition number 213879.

(13) The possibility that **4** is a trifluoroethoxymethyl complex, $[(N\text{-}N)Pt(CH_2OCD_2CF_3)(L)]^+$ (L = TFE-d_3, MeOD), produced by alcoholysis of the C−O bond in a hydroxymethyl complex cannot be ruled out.

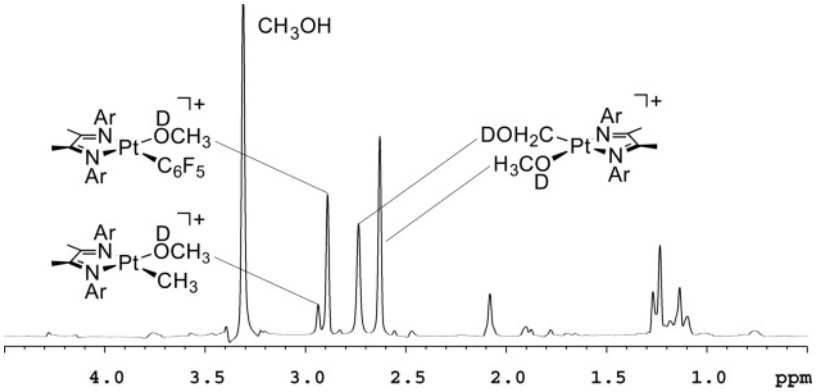

Figure 2. One-dimensional HMQC spectrum for the reaction of **2** with $^{13}CH_3OH$. A solvent presaturation routine was used to minimize the intensity of the free methanol signal at δ 3.3.

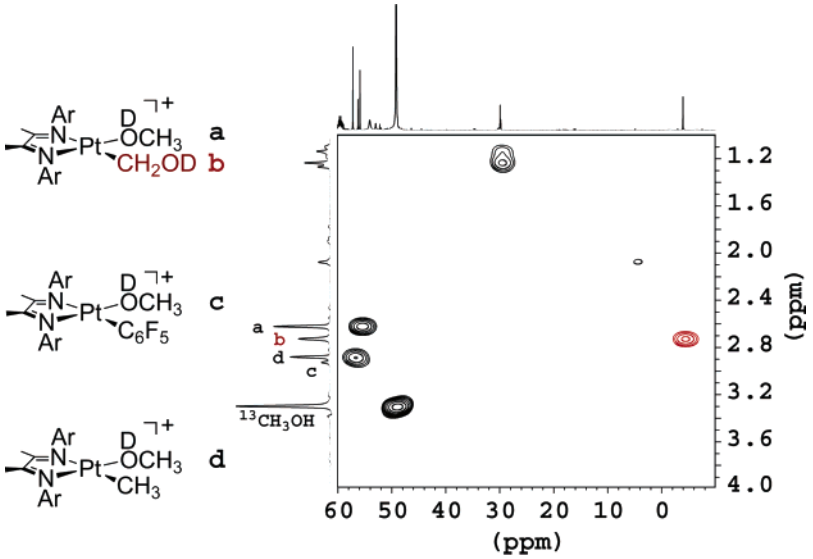

Figure 3. Two-dimensional HMQC for the reaction of **2** with $^{13}CH_3OH$. The 1D HMQC spectrum from Figure 2 as well as a higher-resolution ^{13}C NMR spectrum (both acquired separately) are superimposed on the axes of the 2D plot.

Scheme 5

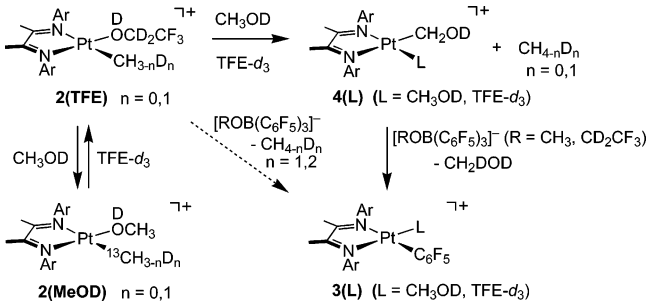

examined by following the disappearance of **2(MeOD)** by ^1H NMR spectroscopy; each reaction exhibited well-behaved pseudo-first-order kinetics. For convenience, usually only [**2(MeOD)**] (the most abundant species) was monitored. Since the equilibrium between **2(MeOD)** and **2(TFE)** is rapidly established—much faster than any conversion of **2** to products—and the reactions are first-order in [**2**], the rate constants thus determined and those that would be obtained by monitoring [**2(TFE)**] (or [$\mathbf{2}_{tot}$]) must be identical. This was verified by comparing rate constants based on [**2(TFE)**] and on [**2(MeOD)**] for experiments with low [MeOD] values (where [**2(TFE)**] is a significant fraction of [$\mathbf{2}_{tot}$]); the results agree to within experimental uncertainty.

Table 2. Kinetics of Methanol-d_1 Activation with **2** at 330 K

[Pt] (M)	[CH_3OD] (M)	[TFE] (M)	k_{obs}(H) (s^{-1})	k_{obs}(H)/α(TFE) (s^{-1})
0.00933	0.123	13.5	0.000136	0.000435
0.00933	0.247	13.4	0.000135	0.000731
0.00949	0.507	13.3	0.000135	0.00137
0.00949	0.738	13.1	0.000132	0.00191
0.00949	1.23	12.8	0.000119	0.00284
0.00949	2.45	12.2	0.000105	0.00518

Table 3. Kinetics of Methanol-d_4 Activation with **2** at 330 K

[Pt] (M)	[CD_3OD] (M)	[TFE] (M)	k_{obs}(D) (s^{-1})	k_{obs}(D)/α(TFE) (s^{-1})
0.00947	0.616	13.2	0.000100	0.00152
0.00933	1.23	12.8	0.0000839	0.00253
0.00890	2.46	12.2	0.0000622	0.00389
0.00949	4.43	11.1	0.0000585	0.00719

The rate constants (k_{obs}) from these first-order plots are shown in Tables 2 and 3, and are plotted against methanol concentration in Figure 4. It can be readily seen that (a) there is a significant kinetic isotope effect (KIE), and (b) the apparent rate constant *decreases* with *increasing* methanol concentration, although not in an inverse first-order manner. Our interpretation of these observations is discussed below.

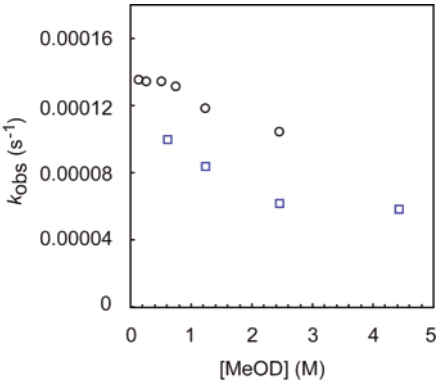

Figure 4. Plot of k_{obs} versus [methanol] for the reaction of **2** with CH_3OD (○) and CD_3OD (□).

Table 4. ^1H and ^{13}C NMR Parameters for **5**[a]

	δ (^1H) (ppm)	$^2J_{HH}$[b] (Hz)	$^4J_{HH}$[c] (Hz)	J_{C-H} (Hz)	δ (^{13}C) (ppm)	J_{Pt-C} (Hz)
CH_{2A}	8.15	5.25	1.74	154.3	133.2	560.2
CH_{2B}	8.01	5.25		153.4	133.2	560.2
CH(OMe)	10.35		1.74	177.7	190.0	637.2
OCH_3	3.79			146.5	67.1	

[a] Acetone-d_6. [b] Geminal coupling between methylidene protons. [c] Coupling of methoxymethylidene proton to *one* methylidene proton.

Reaction of Dimethyl Ether with 2(TFE). As with methanol, addition of anhydrous dimethyl ether (DME) to solutions of **2(TFE)** quickly establishes an equilibrium between the DME-bound platinum cation (**2(DME)**) and **2(TFE)**, again favoring the former, with $K_{eq} = 0.023 \pm 0.002$ at 313 K. Disappearance of the ^1H NMR signals of **2** proceeds slowly at 313 K with the appearance of signals for methane (CH_4 and CH_3D; as with methanol, activation of DME-d_6 gave CH_3D and CH_2D_2 instead), a new species with an unusual spectral pattern (six aromatic ligand resonances instead of the usual four), and small amounts of **3**. On continued monitoring, the new resonances decrease in intensity, at the same time that crystals appear in the NMR tube. The ^1H NMR spectrum of a solution of the isolated crystals in acetone-d_6 exhibits additional resonances downfield of the ligand peaks including one resonance with broad ^{195}Pt satellites. Reaction of **2** with DME-$^{13}C_2$ affords a similar species, allowing full analysis of ^1H and ^{13}C NMR parameters (Table 4). The shifts and splitting patterns of these downfield signals suggest the presence of two alkylidene ligands, one CH_2 group, and one CHX group. This was confirmed by X-ray crystallography, which revealed an unusual structure: a Pt–Pt dimer with μ-CH_2 and μ-$CH(OCH_3)$ groups (**5**, Scheme 6, Figure 5).[14] The molecule is disordered about a center of symmetry; hence only the average Pt–C distance and angles for the μ-CH_2 and μ-$CH(OCH_3)$ groups could be determined (Table 5).

Kinetics of Dimethyl Ether Activation with 2. As with methanol (see above), the disappearance of **2(DME)** was monitored by ^1H NMR at 313 K; it shows pseudo-first-order behavior over more than five half-lives. The dependence of apparent first-order rate constants on [DME] is shown in Table 6 and plotted in Figure 6. A kinetic isotope effect for DME

(14) Crystallographic data have been deposited at the CCDC, 12 Union Road, Cambridge CB2 1EZ, UK and copies can be obtained on request, free of charge, by quoting the publication citation and the deposition number 267189.

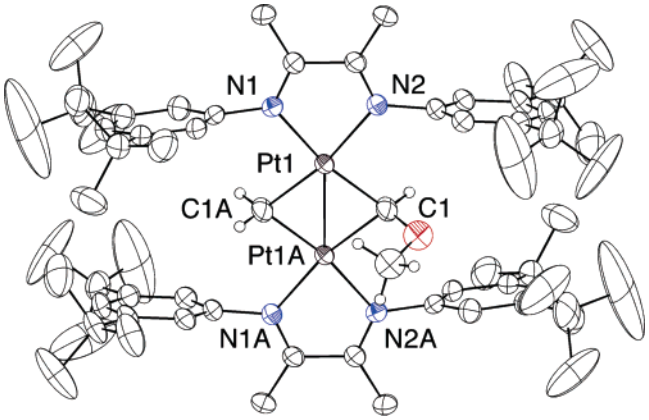

Figure 5. X-ray crystal structure of **5**. Ellipsoids are drawn at 50% probability; the counteranions $[CF_3CD_2OB(C_6F_5)_3]^-$ are not shown.

Scheme 6

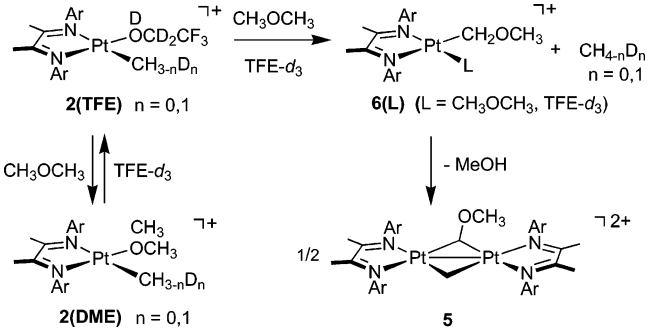

Table 5. Selected Bond Lengths (Å) and Bond Angles (deg) for **5**

Pt1–Pt1A	2.6053(2)
Pt1–C1	2.0055(34)
C1–O1	1.5157(74)
Pt1–C1–Pt1A	81.02(0.13)
C1–Pt1–C1A	98.98(0.13)

Table 6. Kinetics of Dimethyl Ether Activation with **2** at 313 K

[Pt] (M)	[CH_3OCH_3] (M)	[TFE] (M)	k_{obs}(D) (s^{-1})	k_{obs}(D)/α(TFE) (s^{-1})
0.0105	0.163	13.6	0.0000563	0.0000899
0.0105	0.191	13.6	0.0000564	0.0000959
0.0100	0.574	13.2	0.0000987	0.000313
0.00983	0.921	12.9	0.000110	0.000503

activation was determined by a competition experiment: equal amounts of DME-d_0 and DME-d_6 were added to a solution of **2** in an NMR tube, and from the ratio of deuterio and protio isotopologs of the liberated methane, k_H/k_D was measured to be 1.5 ± 0.1.

Discussion

C–H Activation of Methane, Methanol, and Dimethyl Ether. A generalized C–H activation reaction of **2** is shown in eq 1. In the case of RH = methane, this reaction is only observable only by means of isotopic labeling. For methanol and DME, the expected products are hydroxymethyl complex **4** and the analogous methoxymethyl complex **6**, respectively. Very few examples of the former have been characterized; all are octahedral,[15] which would make **4** somewhat unique. Alkoxyalkyl complexes are considerably more common.[16] We therefore anticipated possible difficulties with product stability

Table 7. Crystal and Refinement Data for **5** (CCDC 267189)[a]

empirical formula	$[C_{67}H_{102}N_4OPt_2]^{+2}2(C_{20}H_2BF_{18}O)^-$
formula weight, g/mol	2591.76
crystal size, mm^3	0.29 × 0.25 × 0.18
θ range, deg	2.42 to 34.86
a, Å	12.3114(3)
b, Å	15.4916(4)
c, Å	16.6024(4)
α, deg	63.6320(10)
β, deg	73.3540(10)
γ, deg	88.6650(10)
volume, Å^3	2698.14(12)
Z	1
crystal system	triclinic
space group	$P\bar{1}$
d_{calc}, g/cm^3	1.595
θ range for data collection, deg	1.74 to 40.43
completeness to $\theta = 40.43°$	87.30%
reflections collected	74339
independent reflections	29995 [$R_{int} = 0.0603$]
absorption correction	SADABS ($\mu = 2.703$ mm^{-1})
max. and min. transmission	1.000000 and 0.831789
goodness-of-fit on F^2	1.748
R indices (all data)	$R_1 = 0.1021$, $wR_2 = 0.1148$

[a] At 100(2) K. [b] $R_1 = \Sigma||F_o| - |F_o||/\Sigma|F_o|$. [c] $wR_2 = [\Sigma[w(F_o^2 - F_c^2)^2]/\Sigma[w(F_o^2)^2]]^{1/2}$.

for the reaction of methanol, but less so for DME. In fact, it is just the other way around. Hydroxymethyl complex **4** is indeed unstable to reaction conditions, reacting with a pentafluorophenyl group from the counteranion to give **3** (which is also produced directly from **2**; see below) and hence could not be isolated. However, it can be detected by NMR and, under the right conditions, is present in sufficient concentration to permit full characterization by 1D and 2D ^{1}H and ^{13}C NMR spectroscopy.

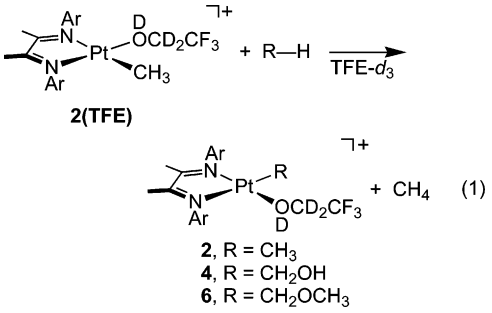

In contrast, no evidence for any methoxymethyl complex **6** could be detected in the reaction of DME; the only product observed (besides small amounts of **3**) is the novel methylene/methoxymethylene-bridged dimer **5**. There are previous reports wherein proposed α-alkoxyalkyl intermediates generated by C−H activation of tetrahydrofuran or diethyl ether result in the formation of Fischer carbene hydride complexes by α-elimination.[17] An analogous step here, followed by formation of a hydride-bridged dimer and loss of methanol, would lead to **5**

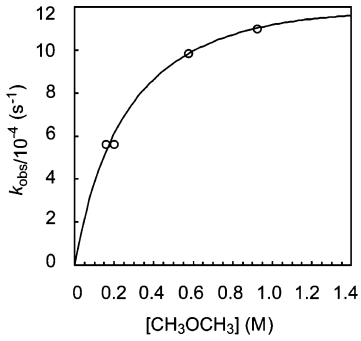

Figure 6. Plot of k_{obs} versus [DME] for the reaction of **2** with CH_3OCH_3.

Scheme 7

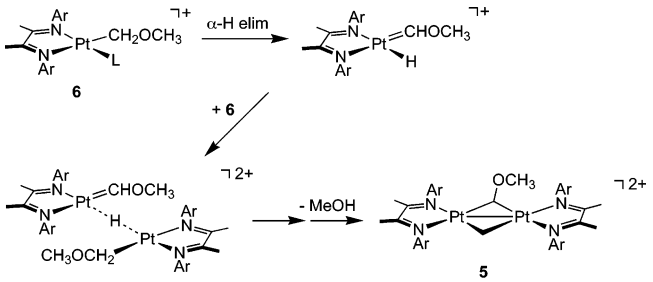

(Scheme 7). Alternatively, methanol loss could be an early step in the mechanism; α-alkoxyalkyl ligands have been shown to undergo C−O bond cleavage in the presence of strong acids.[16] At present, we cannot distinguish between these (or other) possibilities, nor explain why **4** is relatively stable and exhibits no such reactivity.

The bonding in **5** is unusual. The diamagnetism of the dicationic complex and the short Pt−Pt distance (2.6053(2) Å) suggest formulation as a Pt(III)−Pt(III) dimer with a metal−metal bond, analogous to the only other examples of hydrocarbyl-bridged platinum−platinum dimers.[18] The ^{1}H and ^{13}C spectroscopic parameters of **5** also provide some insight. The downfield chemical shifts of the bridging groups in both the ^{1}H and ^{13}C spectra are most likely due to a large paramagnetic contribution, more typically characteristic of terminal alkylidene ligands. The large C−H coupling constants for both bridges—especially the methoxymethylidene—and small platinum−carbon coupling constants suggest high s-character in the C−H bonds and larger p-orbital contributions to the C−Pt bonds that may arise from the acute Pt−C−Pt bond angles and the electron-deficient nature of the platinum center.

Despite the fact that neither **4** nor **6** is stable, the initial reaction of **2** with both methanol and DME is clearly C−H activation, as methane is liberated during reaction of perdeuterated substrate with one more deuterium than with unlabeled substrate. Furthermore, since clean pseudo-first-order disappearance of platinum methyl complex **2** is observed in every experiment, the instability of **4** (gradual) or **6** (immediate) must not have any effect on the kinetic parameters determined by that method. (The *competing* formation of **3** from **2** does affect the kinetics, of course, as discussed in the following section.)

Kinetics of C−H Activation: Substrate Inhibition. The kinetics of methane activation, as determined from disappear-

(15) (a) Thorn, D. L.; Tulip, T. H. *Organometallics* **1982**, *1*, 1580−1586. (b) Blackmore, T.; Bruce, M. I.; Davidson, P. J.; Iqbal, M. Z.; Stone, F. G. A. *J. Chem. Soc. A* **1970**, 3153. (c) Casey, C. P.; Andrews, M. A,; McAlister, D. R.; Rinz, J. E. *J. Am. Chem. Soc.* **1980**, *102*, 1927. (d) Sweet, J. R.; Graham, W. A. G. *J. Organomet. Chem.* **1979**, *173*, C9. (e) Headford, C. E. L.; Roper, W. R. *J. Organomet. Chem.* **1980**, *198*, C7. (f) Espenson, J. H.; Bakac, A. *J. Am. Chem. Soc.* **1981**, *103*, 2721 and references therein.
(16) Thorn, D. L. *Organometallics* **1986**, *5*, 1897−1903 and references therein.
(17) (a) Holtcamp, M. W.; Labinger, J. A.; Bercaw, J. E. *J. Am. Chem. Soc.* **1997**, *119*, 848−849. (b) Luecke, H. F.; Arndtsen, B. A.; Burger, P.; Bergman, R. G. *J. Am. Chem. Soc.* **1996**, *118*, 2517−2518.
(18) (a) Uson, R.; Fornies, J.; Tomas, M.; Casas, J. M.; Cotton, F. A.; Falvello, L. R. *J. Am. Chem. Soc.* **1985**, *107*, 2556. (b) Uson, R.; Fornies, J.; Tomas, M.; Casas, J. M.; Cotton, F. A.; Falvello, L. R.; Llusar, R. *Organometallics* **1988**, *7*, 2279. (c) Uson, R.; Fornies, J.; Tomas, M.; Casas, J. M.; Cotton, F. A.; Falvello, L. R.; Feng, X. *J. Am. Chem. Soc.* **1993**, *115*, 4145.

ance of ^{13}C-labeled **2**, are straightforward: there is a linear dependence on methane concentration (Figure 1), with the small positive intercept corresponding reasonably well to the rate of decomposition in the absence of added substrate.

In contrast, C−H activation rates for both methanol and DME exhibit nonlinear dependence on substrate concentration (Figures 4 and 6). We attribute this to inhibition by substrate coordination. We have previously shown that benzene C−H activation in TFE solution is inhibited by water because the aquo-platinum methyl cation (**2(H$_2$O)**) is thermodynamically favored over (by a factor of 430) but much less reactive than the TFE-ligated cation **2(TFE)**; the kinetics indicate that the latter is the *sole* reactive C−H activating species.[11a,d] NMR studies show that methanol and DME also coordinate to the platinum center more tightly than TFE, by factors of 240 and 44, respectively.

Assuming that, as for water, the more tightly bound MeOR (R = D, Me) cannot be directly displaced by the substrate's C−H bond, productive C−H activation of methanol and DME will likewise proceed only via a bimolecular reaction between substrate and **2(TFE)**. The expected rate law is derived in eqs 2−6; the observed pseudo-first-order rate constants will be of the form $k_{obs} = k_2[\text{MeOR}]\alpha_{TFE}$, where α_{TFE} is the mole fraction of total **2** present as **2(TFE)**.

$$\textbf{2(MeOR)} + \text{TFE} \overset{K_{eq}}{\rightleftharpoons} \textbf{2(TFE)} + \underset{(\text{R} = \text{D, Me})}{\text{MeOR}} \quad (2)$$

$$\textbf{2(TFE)} + \text{MeOR} \xrightarrow{k_2} \text{products} \quad (3)$$

$$K_{eq} = \frac{[\textbf{2(TFE)}]\cdot[\text{MeOR}]}{[\textbf{2(MeOR)}]\cdot[\text{TFE}]} \quad (4)$$

$$[\text{Pt}_{tot}] = [\textbf{2(TFE)}] + [\textbf{2(MeOR)}] = [\textbf{2(TFE)}]\cdot\left(1 + \frac{[\text{MeOR}]}{K_{eq}[\text{TFE}]}\right) \quad (5)$$

$$-\frac{d[\text{Pt}]}{dt} = k_{obs}[\text{Pt}_{tot}] = k_2[\textbf{2(TFE)}]\cdot[\text{MeOR}] \quad (6)$$

$$k_{obs} = k_2[\text{MeOR}]\cdot\alpha_{TFE} = k_2[\text{MeOR}]\cdot\frac{1}{1 + \frac{[\text{MeOR}]}{K_{eq}[\text{TFE}]}} \quad (7)$$

The dependence of observed rate constant on [MeOR] predicted from the rate law of eq 7 is saturation kinetics; the rate should increase linearly from zero [MeOR] and then level off as the platinum complex is almost completely sequestered in its unreactive MeOR-bound form. Just such behavior is observed for the C−H activation of DME (Figure 6). A plot of the observed rate constants corrected for the concentration of **2(TFE)** at each point (k_{obs}/α_{TFE}), where α_{TFE} is calculated from the concentrations of TFE and DME, and the equilibrium constant measured by NMR (see Table 6) versus [DME] should be linear, as it is (Figure 7); there is a negligible intercept. The second-order rate constant for DME C−H activation determined from this plot is $k_2 = 5.4 \pm 0.5 \times 10^{-4}$ M^{-1} s^{-1}.

An alternative mechanism could be invoked, in which C−H activation of methanol and/or DME proceeds directly from the corresponding substrate-bound cation (**2(MeOD)** or **2(DME)**) via intramolecular β-hydride elimination. Such a process was

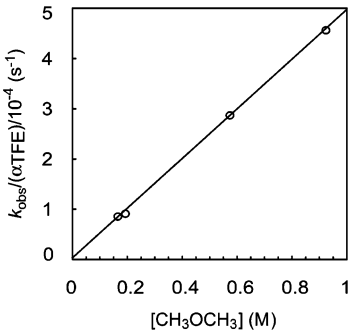

Figure 7. Plot of k_{obs}/α_{TFE} versus [DME] for the reaction of **2** with CH_3OCH_3.

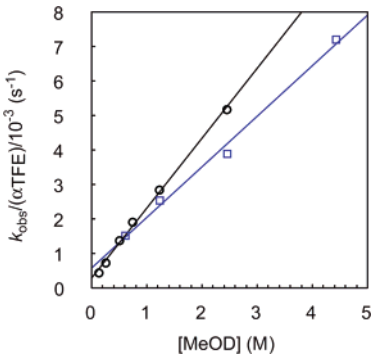

Figure 8. Plot of k_{obs}/α_{TFE} versus [methanol] for the reaction of **2** with CH_3OD (○) and CD_3OD (□).

implicated in the activation of a C−H bond of diethyl ether by a related Pt(II) complex.[17a] However, such a route is not consistent with the observed substrate dependence in the case of DME. Saturation kinetics would be expected, in *qualitative* agreement with Figure 6, but given the value of K_{eq} determined by NMR, saturation would be reached at a much lower [DME] value than observed. (The value of K_{eq} calculated by fitting the data of Table 6 to the rate law of eq 7 (shown in Figure 6) is essentially identical to that measured by NMR.)

On the other hand, the apparent rates of disappearance of **2** in methanol C−H activation do not fit the expected concentration dependence. Instead, the rate is highest at low methanol concentrations and decreases modestly as the concentration increases (Figure 4). If we process the data (as we did for DME) according to eq 7 (Tables 2, 3, and 6), the plot of apparent rates corrected for α_{TFE} *does* show a linear dependence on the substrate concentration, but with a substantial nonzero intercept (Figure 8). How are these to be explained?

The large intercept, which corresponds to the unexpectedly high values of the observed rate at low methanol concentrations, indicates a parallel path for consuming **2(TFE)**. This must be the pentafluorophenylation of **2(TFE)** to give **3**, which is observed in all samples, but is especially prominent in methanol activation. The linear fit of the corrected rate constants (k_{obs}/α_{TFE}) to the methanol concentration over a wide range strongly implies that this decomposition path is also subject to substrate inhibition; that is, both the C−H activation and the decomposition to **3** proceed only from **2(TFE)**.

According to this mechanism (see Scheme 8), where both the productive methanol activation as well as the parallel decomposition of **2** to **3** depend on [**2(TFE)**], the rate expression

Scheme 8

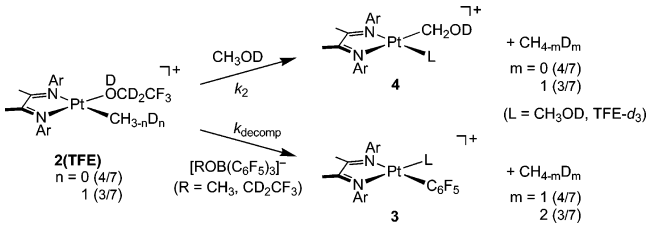

can be modified to include a term for the pentafluorophenylation rate (k_{decomp}) as shown in eq 8. After correcting for α_{TFE} as before (Tables 2 and 3), both rate constants may be calculated from the slope (k_2) and intercept (k_{decomp}) of the plot in Figure 8, yielding the following parameters (at 330K): $k_2(CH_3OD) = 2.0 \pm 0.2 \times 10^{-3}\ M^{-1}\ s^{-1}$, $k_H/k_D = 1.4 \pm 0.1$, $k_{decomp} = 2 \pm 1 \times 10^{-4}\ s^{-1}$.

$$k_{obs} = (k_2[\mathrm{MeOR}] + k_{decomp}) \cdot \frac{1}{1 + \dfrac{[\mathrm{MeOR}]}{K_{eq}[\mathrm{TFE}]}} \qquad (8)$$

Including the parallel decomposition path in the rate expression has a dramatic impact on the expected [methanol] dependence of the uncorrected, observed rates. Instead of simple saturation dependence, the observed rate will be a sum of two terms—C−H activation and decomposition—in which the first saturates while the second falls off as [methanol] increases.[19] This is shown in Figure 9, where the calculated C−H activation ($k_{obs-C-H} = k_2[\mathrm{MeOD}](\alpha_{TFE})$) and pentafluorophenylation ($k_{obs-C_6F_5} = k_{decomp}(\alpha_{TFE})$) rates and their sum are plotted as a function of [methanol], along with the measured first-order rate constants for the disappearance of the starting material. The agreement is quite good at higher [methanol] levels, but not for low [methanol] (see the following section for discussion).

According to this interpretation, decomposition dominates at low [methanol] and methanol C−H activation at high [methanol]. Independent support of a change in the dominant reaction path is provided by observation of variable isotopic composition of the liberated methane. Recall that **2** contains approximately equal amounts of CH_3 and CH_2D groups, so that methane produced by methanol-d_1 C−H activation (in CF_3CD_2OD) will carry a *protium* from the substrate yielding CH_4 and CH_3D, whereas the methane produced in pentafluorophenylation receives an additional *deuterium* from the solvent yielding CH_3D and CH_2D_2 (Scheme 8). Accordingly, at low [methanol], the methane should be mostly CH_3D and CH_2D_2, from decomposition to **3**, while at higher [methanol], there should be much less CH_2D_2 and more CH_4, as observed.

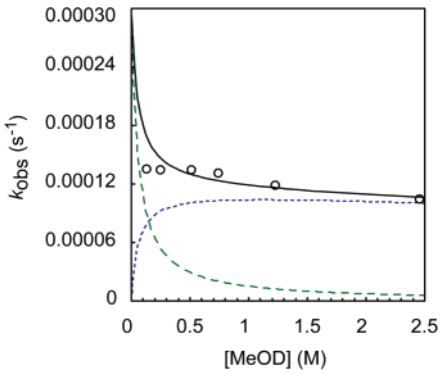

Figure 9. Observed first-order rate constants for the reaction of **2** with CH_3OD (□) and calculated C−H activation ($k_2 \times [\mathrm{MeOD}] \times \alpha_{TFE}$) (- - -) and pentafluorophenylation ($k_{decomp} \times \alpha_{TFE}$) (— — —) rate constants based on eq 8.

Pentafluorophenyl Transfer Rates. 3 is formed, in varying amounts, in all of the reactions examined here. **2** reacts directly with the pentafluorophenylating agent to give **3**, in competition with substrate activation; also **4**, the initial product of methanol activation, undergoes subsequent conversion to **3**. Higher concentrations of $\mathbf{[2]^+[CF_3CD_2OB(C_6F_5)_3]^-}$ generally give rise to faster decomposition to **3**, as would be expected for first-order dependence on the concentrations of both platinum and borane, second-order overall. Exposure of solutions to water also accelerates formation of **3**.

The kinetics for methanol activation, however, show complexities in the decomposition process, even at constant [Pt]. The decomposition rate constant calculated from the intercept of the plot in Figure 8 ($2 \pm 1 \times 10^{-4}\ s^{-1}$) is 5 times larger than that observed in the absence of substrate ($4 \times 10^{-5}\ s^{-1}$ (330 K)). Furthermore, as noted above (see Figure 9), the observed rate of disappearance of **2** at low methanol concentrations (which is largely decomposition to **3**) is significantly less than that predicted from the kinetic parameters obtained from Figure 8. We interpret these observations in terms of an equilibrium between two different borate anions, $[(CF_3CD_2O)B(C_6F_5)_3]^-$ and $[(CH_3O)B(C_6F_5)_3]^-$, with the latter being a significantly more potent pentafluorophenyl transfer agent.[20] At low [methanol] (on the same order as that of $B(C_6F_5)_3$, which is added in a 2:1 ratio to [**2**]), the less reactive trifluoroethoxyborate dominates, resulting in a decomposition rate slower than expected from extrapolation of the results at higher [methanol]. The difficulty of drying methanol thoroughly is also a likely contributor to this behavior, as water has been seen to accelerate decomposition. The presence of different amounts of water may explain the difference between the intercepts in the activation of methanol-d_4 and methanol-d_1 (Figure 8). The reactions of DME show no such complications, as (dry) DME would not be expected to form more reactive adducts with the borane, although as noted above, **6** decomposes comparatively more rapidly via a separate pathway, namely, loss of methanol and dimerization to **5**.

We attempted a better fit of the dependence of k_{obs} on [methanol] by including two additional parameters—the equilibrium between the two borates and a second k_{decomp}—but obtained only a modest improvement to the fit at low [methanol]. It is important to note, however, that this variation in the parallel decomposition path has a minimal impact on the calculated rate constant for methanol C−H activation. That value is extracted from the slope of the line in Figure 8, which is primarily determined by the high [methanol] points, where C−H activation is dominant, and is relatively insensitive to the low [methanol] points.

On the other hand, it must be acknowledged that if the low [methanol] points are left out of the analysis, the possibility of

(19) It can be seen from eq 6 that the rate can also fall off when [methanol] is sufficiently high that [TFE] decreases significantly; however, the data in Tables 5 and 6 show that this factor alone cannot account for the magnitude of the rate decrease.

(20) In Suzuki couplings, which similarly involve transfer of organic groups from boron to transition metal centers, the transmetalating boronic acids can be activated by anions. See: Miyaura, N.; Suzuki, A. *Chem. Rev.* **1995**, *95*, 2457−2483.

Scheme 9

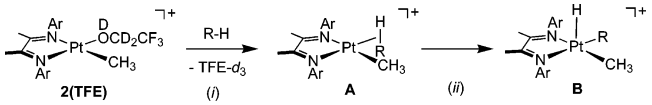

intramolecular activation of coordinated methanol remains open. One could envision **2(MeOD)** undergoing β-H abstraction to eliminate methane and generate a protonated formaldehyde complex, which, on addition of TFE or methanol, would open to **4(L)**, while **2(TFE)** would decompose to **3** as before. The resulting rate law (eq 9) would be consistent with the linear dependence of k_{obs} on α_{TFE} observed for the high [methanol] points in Figure 8. We feel this scenario is much less likely on a number of grounds. The rate constant calculated for methanol in the proposed mechanism (Scheme 8) is quite similar to that for DME (after correcting for temperature; see below); there is no obvious reason why methanol and DME should follow different routes; it is far from clear whether an elimination–rearrangement sequence could lead to **4**. Nonetheless, in contrast to the DME case (see above), this alternative reaction scheme cannot be dismissed on the basis of the kinetics alone.

$$k_{obs} = k_{decomp}\cdot\alpha_{TFE} + k_2\cdot(1 - \alpha_{TFE}) = \alpha_{TFE}\cdot(k_{decomp} - k_2) + k_2 \quad (9)$$

Isotope Scrambling and the Reversibility of C–H Activation. As noted in the Introduction, C–H activation is typically a multistep process, with reversibility and the identity of the rate-determining step often at issue. The first two steps in C–H activation by **2** (Scheme 9) are displacement of the coordinated solvent by substrate (***i***), leading to an alkane σ-complex (**A**), followed by oxidative cleavage of the coordinated C–H bond (***ii***), to generate a platinum(IV) alkyl hydride (**B**) that goes on to reductively eliminate methane (not shown).[11] In principle either ***i*** or ***ii*** might be the rate-determining step; previous studies in our group on arene activation (where the detected intermediate is a π-complex rather than **A**) have provided examples of both.[11a] Because **A** is also an intermediate in the protonolysis of **1**, we can deduce from the observed statistical isotopic scrambling in that process (see above) that displacement of methane from **A** is slow compared with the rapid and reversible C–H bond cleavage and forming steps (Scheme 10). Similarly, activation of C_6D_6 by analogues of **2** gives complete isotopic scrambling between phenyl and methyl sites in cases where step ***i*** is rate-determining.[11a,21]

In the activation of methane, then, by microscopic reversibility, coordination of the substrate is the slowest, rate-determining step, as shown in the qualitative reaction coordinate in Figure 10. By symmetry, loss of the labeled and unlabeled methyl groups from intermediate **B** is equally likely; hence the rate determined by disappearance of the labeled starting material is only half the actual rate of methane activation. Accordingly, the second-order rate constants given in Table 1 are twice the apparent values.

In contrast, activation of methanol-d_4 or dimethyl ether-d_6 transfers only a *single* deuterium from the substrate to the liberated methane, implying one or more irreversible steps leading to formation of products. This irreversibility is important to the kinetics analysis because it means that every time methanol or dimethyl ether reacts with **2** to form a σ-complex the reaction continues to completion. Hence the correction factor of 2 applied to methane activation is not appropriate in these cases. This irreversibility can be accounted for by a lowered barrier to loss of methane from the species corresponding to structure **A′** in Figure 10 (note that the reaction coordinate is no longer symmetrical for activation of any substrate other than methane). Methane decoordination might be facilitated by simple steric destabilization or a more specific intramolecular displacement by the pendant oxygen atom of the hydroxymethyl or methoxymethyl group.

Alternatively, it is conceivable that C–H bond cleavage (step ***ii***) becomes rate-determining for these substrates, but there is no obvious reason that should be so. Furthermore, KIEs for methanol and DME activation are small and normal, approximately 1.4–1.5. Comparison to the much larger values (KIE = 4–5) found for the oxidative cleavage of various alkane C–H bonds at titanium and rhodium[9,10] suggests that, as in the methane reaction, C–H bond coordination rather than bond breaking is rate-determining. Several studies of *equilibrium* isotope effects for C–H versus C–D coordination report values in the range of 1.2–2, indicating only modest weakening of the bond in the σ-complex;[22,23] since relatively less bond weakening would be expected in the transition state leading to coordination, small normal KIEs seem reasonable. Few measurements of KIEs for C–H coordination have been documented. Competition experiments for reaction at iridium give values in this range for *n*-hexane (KIE = 1.2)[24] and cyclohexane (KIE = 1.38).[25] While it is not certain that these represent C–H coordination, the relative activation rates of linear alkanes depend on the number of secondary C–H bonds, suggesting that coordination rather than C–H bond cleavage is indeed rate-determining. A recent paper reports a KIE of 3.3 for the oxidative addition of cyclohexane to a rhodium center, but whether this reflects coordination or C–H cleavage (or a composite of both) could not be determined.[9d] Preliminary studies on the reaction of cyclohexane with **2** yield KIE = 1.3; isotope scrambling patterns suggest that C–H coordination is rate-determining.[26]

These considerations strongly suggest that C–H coordination is rate-determining for all three substrates studied here, methanol and DME as well as methane, and that the irreversibility for the first two (manifested by the absence of isotopic scrambling) is a consequence of accelerated methane loss. We have previously suggested that C–H coordination will be rate-determining for reactions of aliphatic C–H bonds at platinum even for cases where aromatic C–H cleavage becomes rate-determining because of the poorer coordinating ability (and consequent higher transition-state energy for substitution) of C–H σ-bonds compared to C=C π-bonds.[27] It should be noted, though, that some unusually large *inverse* EIEs (12–14) have been reported for the binding of alkanes to [Cp′Rh(CO)] in liquid krypton at 165 K.[10] A substantial inverse EIE effect on

(21) See also: Heiber, H.; Johansson, L.; Gropen, O.; Ryan, O. B.; Swang, O.; Tilset, M. *J. Am. Chem. Soc.* **2000**, *122*, 10831–10845.

(22) Lawes, D. J.; Geftakis, S.; Ball, G. E. *J. Am. Chem. Soc.* **2005**, *127*, 4134–4135.
(23) Calvert, R. B.; Shapley, J. R. *J. Am. Chem. Soc.* **1978**, *100*, 7726–7727.
(24) Periana, R. A.; Bergman, R. G. *J. Am. Chem. Soc.* **1986**, *108*, 7332–7346. See especially ref 10.
(25) Janowicz, A. H.; Bergman, R. G. *J. Am. Chem. Soc.* **1983**, *105*, 3929–3939.
(26) Chen, G. C.; Labinger, J. A.; Bercaw, J. E. Unpublished results.
(27) See the Supporting Information to ref 14d for a discussion.

Scheme 10

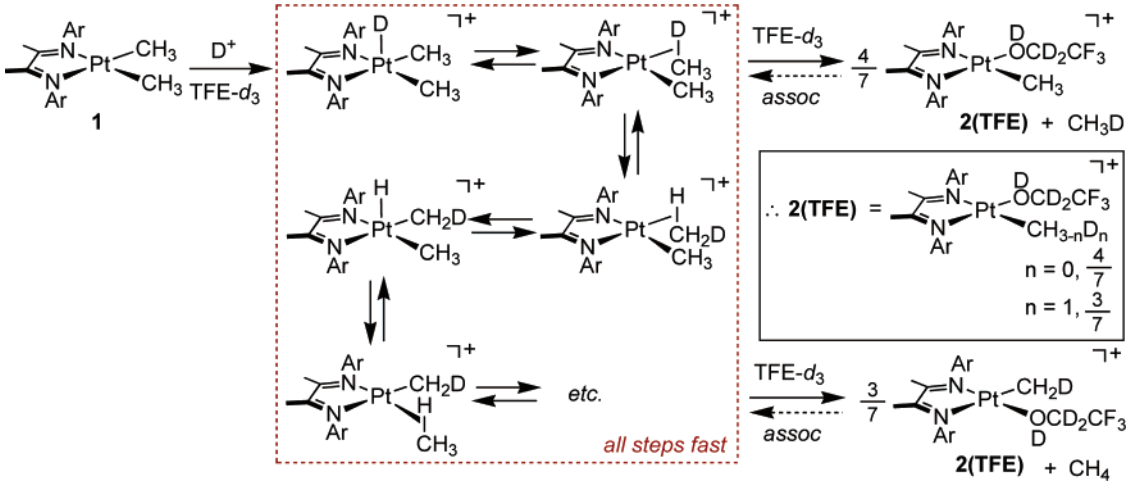

the preequilibrium binding of substrate followed by rate-determining C−H oxidative cleavage with a slightly larger normal KIE could give an apparent KIE in the range observed. While such a scenario seems less probable, it cannot be ruled out at this time.

Conclusions: Substrate Selectivity. The relative rates of methane, methanol, and DME C−H activation show that the platinum center is relatively unselective: $k_{methane}/k_{methanol} = 1/1.3$, 330 K; and $k_{methane}/k_{dimethyl\ ether} = 1/2$, 313 K. These values all appear to represent rates of displacement of solvent by the substrate's C−H bond. The low selectivities in this model system are consistent with those inferred from the behavior of the "real" Shilov system (see above) and suggest that C−H coordination is probably rate-determining there, as well. Consistent with that suggestion, it has been found that during catalytic H/D exchange at Pt(II) (in the absence of an oxidant) there is multiple exchange during each C−H activation event.[7e] (This result should be interpreted with caution, however, because Pt(0), which can form under these conditions, efficiently scrambles H with D.)

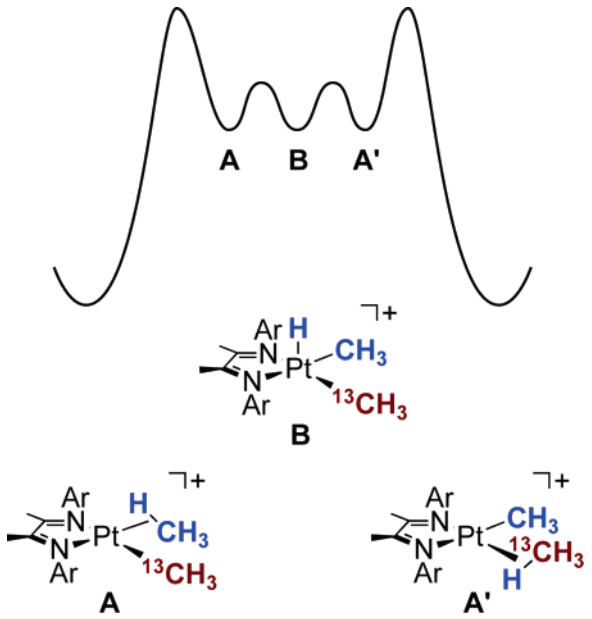

Figure 10. Qualitative potential energy surface for the reaction of **2** with methane.

In light of the relatively small difference between the reactivity of methane and methanol, it is somewhat surprising that we have never detected any reaction of the C−H or C−D bonds of trifluoroethanol with these cationic Pt(II) complexes (a fact that is, of course, crucial to its utility as solvent for these model studies). From the high concentration of TFE and the absence of any NMR-detectable (<5%) product of its activation, we estimate an upper limit on reactivity for the C−H bond of TFE of 1/100 that of methane, methanol, and DME. Presumably, this is a result of the additional electron-withdrawing effect of the trifluoromethyl group, which must destabilize the σ-complex (or, more precisely, the transition state leading to it) by >2−3 kcal/mol. A major role for steric effects is harder to argue since the van der Waals radius of fluorine (1.47 Å) is only slightly larger than that of hydrogen (1.35 Å).[28]

Even more interesting is the high selectivity of the Periana system for the oxidation of methane over methyl bisulfate (~100:1).[2c] It is not known whether the rate-determining step in that system is the same as in our models, but one might imagine that the electron-withdrawing capacity of the bisulfate group works in concert with its "neopentyl-like" steric influence to disfavor methyl bisulfate relative to methane activation. These conclusions point to the importance of the fuming sulfuric acid solvent in the Periana system. Under these conditions, the formation of the methane oxidation product as a "protected" form of methanol is clearly crucial; the electronic effect of simple hydroxy (or methoxy) substitution is not sufficient alone to influence the relative rate of C−H bond coordination so strongly. The only example of strong (7:1) preference for activation of methane over methanol is found for a dimeric Rh(porphyrin) system, where the large KIEs (9−11) point to C−H bond cleavage as the rate-limiting step, and kinetics implicate a trimolecular transition state that would be expected to be subject to strong steric influence.[29]

As noted in the Introduction, the potential yield of a methane oxidation product, such as methanol, is constrained by relative reactivities. In a case such as that studied here, where the solvent form of the activating complex is less stable but more reactive than the methanol-bound form, the rate of methane activation will decrease as [methanol] increases, whereas that of methanol

(28) Slater, J. C. *J. Chem. Phys.* **1964**, *41*, 3199.
(29) Cui, W.; Zhang, P. Wayland, B. B. *J. Am. Chem. Soc.* **2003**, *125*, 4994−4995.

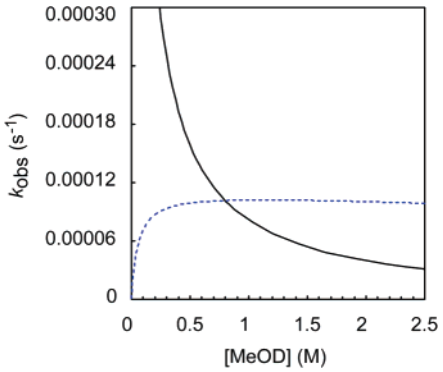

Figure 11. Comparison of the apparent first-order rate constants for C−H activation of methane (solid line, at constant [methane] = 1.0 M) and methanol (dashed line) by **2**.

activation will level off. This is illustrated for the case of **2** in Figure 11, where the apparent pseudo-first-order rate constants for the two process (neglecting any contribution from the decomposition to **3**) are calculated as a function of [methanol] from the kinetic parameters derived above. It is clear that with relative reactivities on this order, it would be necessary to keep the methanol concentration low, perhaps by some process that permits continual removal as it is formed.

Current ongoing work in our group is aimed at extending these findings to C−H bonds in a wider range of hydrocarbons and functionalized hydrocarbons.

Experimental Section

General Methods. All air and/or moisture-sensitive compounds were manipulated using standard Schlenk techniques or in a glovebox under a nitrogen atmosphere, as described previously.[30] **1** was prepared as described previously[11a] and purified by filtering a saturated methylene chloride solution followed by precipitation of the platinum complex at −78 °C. The dark purple solid was stored under high vacuum for 3 days to remove cocrystallized solvent molecules and then in a P_2O_5 desiccator in the glovebox. $B(C_6F_5)_3$ was sublimed at 90 °C in vacuo and stored in a P_2O_5 desiccator in the glovebox. All deuterated solvents and ^{13}C-labeled compounds were purchased from Cambridge Isotope Laboratories, with the exception of dimethyl ether-$^{13}C_2$, which was purchased from Isotec. Methanol-d_1 and methanol-d_4 were stored over 3 Å molecular sieves and then distilled from sodium. Trifluoroethanol-d_3 was dried over 3 Å molecular sieves for at least 5 days and then was vacuum distilled onto $B(C_6F_5)_3$ and shortly thereafter distilled into a Strauss flask and stored in the glovebox. Ultrahigh purity methane (99.95%) was purchased from Matheson and stored over activated alumina prior to use. Dimethyl ether was purchased from Matheson and stored as a solution in tetraglyme over sodium and benzophenone at <1 atm of vapor pressure for at least 1 week prior to its use. NMR spectra were recorded on Varian Mercury 300, Varian INOVA 500, and Varian Innova 600 spectrometers.

[(μ-SMe$_2$)Pt($^{13}CH_3$)$_2$]. [(μ-SMe$_2$)Pt($^{13}CH_3$)$_2$] was prepared similarly to the unlabeled version[31] using $^{13}CH_3$Li·LiI (prepared from $^{13}CH_3$I and LiBu^t in pentane). The reaction mixture and product were slightly darker than usual, so the product was dissolved in THF and additional carbon was added. The suspension was filtered, and the product reprecipitated with petroleum ether at −78 °C. This procedure was repeated a second time, finally yielding 1.09 g (49% based on platinum) of white powder. ^1H NMR (300 MHz, C_6D_6): δ = 1.00 (m, J_{C-H} = 128.1 Hz, J_{Pt-H} = 87.53 Hz, 12H), 2.05 (s, J_{Pt-H} = 20.32 Hz, 12H). ^{13}C NMR (75.4 MHz, C_6D_6): δ = −6.41 (J_{Pt-C} = 791.7 Hz).

[(N-N)Pt($^{13}CH_{3-n}D_n$)(DOCD$_2$CF$_3$)]$^+$[CF$_3$CD$_2$OB(C$_6$F$_5$)$_3$]$^-$ (2-^{13}C-(TFE)) was prepared as previously described for the unlabeled compound.[11d] The ^1H NMR signal for the Pt−CH_3 group (at δ = 0.74 ppm) appeared as a doublet, $^1J_{C-H}$ = 128.3 Hz; the corresponding value for $^1J_{C-D}$ = 19.5 Hz was determined from the ^{13}C NMR signal for the Pt−CH_2D group (δ = −8.6 ppm).

Kinetics of Methane Activation. Stock solutions of **2-^{13}C(TFE)** were prepared by weighing **1-$^{13}C_2$** and tris(pentafluorophenyl)borane (2 equiv) into 5.0 mL volumetric flasks and adding TFE-d_3 (approximately 3 mL). The suspension was mixed by shaking until the solids had dissolved. Additional TFE-d_3 was added to dilute the sample to 5.0 mL, the solution mixed and then transferred to a vial and stored at −30 °C in the glovebox freezer. Solutions prepared from anhydrous reagents in this way are stable for days, with minimal decomposition (∼5−10%) after 1 week; 400 μL of solution was measured into a sapphire NMR tube using a volumetric syringe, the cap tightly closed and the sample taken to the high-pressure manifold. After evacuating the manifold, the tube was charged with the desired pressure of dry methane gas, and the tube inserted in the NMR spectrometer that had been preheated to 330 ± 0.5 or 313 ± 0.5 K as determined by an ethylene glycol temperature calibration standard. After allowing the sample to reach the probe temperature (5 min), the tube was removed, mixed by rocking, and reinserted into the probe. The ^1H NMR spectrum was recorded to measure the methane concentration versus the known concentration of platinum in the solution. Kinetics were monitored by following the peak height of the ^{13}C-labeled platinum methyl signal in the ^{13}C NMR; parallel determinations using integrated peak areas gave very similar, though somewhat noisier, results. After the run, the sample height was measured to ±0.5 mm and compared with the starting height to correct the concentration for the change in volume due to the dissolved gas.

CAUTION: Handling high pressures of gas in sapphire NMR tubes is extremely dangerous and should be approached with caution. Many steps were taken to minimize exposure to the tubes while under pressure. The tubes and high-pressure manifold used in this work were tested regularly at pressures well above those employed under working conditions.

Reaction of 2 with Methanol. Addition of MeOD to solutions of **2(TFE)** in TFE resulted in the immediate generation of a new set of NMR signals corresponding to **2(MeOD)**: ^1H NMR (600 MHz, TFE-d_6) δ = 0.75 (s, 3H), 1.35 (s, 9H), 1.37 (s, 9H), 1.81 (s, 3H), 2.02 (s, 3H), 3.04 (s, 3H), 6.84 (s, 2H), 7.06 (s, 2H), 7.52 (s, 1H), 7.60 (s, 1H); the equilibrium constant relating the two solvated complexes was determined from the relative peak intensities as a function of [MeOD]. On prolonged standing at room temperature (faster at 330 K), the NMR signals for **2** were replaced by those for **3** and (in some cases) **4**, as described in the Results section.

Kinetics of Methanol Activation. Stock solutions were made by weighing **1** and tris(pentafluorophenyl)borane (2 equiv) into 1.0 mL volumetric flasks and adding TFE-d_3 (approximately 0.5 mL). The suspension was shaken until all solids had dissolved. After the solids had dissolved, the desired amount of methanol was added with a microliter syringe followed by enough TFE-d_3 to dilute to 1.0 mL total volume. The concentration of TFE was calculated from its known density, assuming the volumes of TFE and methanol are additive; 700 μL was measured into a J. Young NMR tube using a volumetric syringe, the cap tightly closed and the tube inserted in the NMR spectrometer that had been preheated to 330 ± 0.5 K. Kinetics were monitored by following the disappearance of the starting material in the ^1H NMR spectrum.

Reaction of 2 with Dimethyl Ether. Dimethyl ether was distilled from Na/benzophenone in tetraglyme into a liquid nitrogen-cooled receiver. Frozen DME was maintained under vacuum to remove any volatiles and condensed into a degassed J. Young tube containing 0.7

(30) Burger, B. J.; Bercaw, J. E. In *New Developments in the Synthesis, Manipulation, and Characterization of Organometallic Compounds*; Wayda, A., Darensbourg, M. Y., Eds.; American Chemical Society: Washington, D.C., 1987; Vol. 357.
(31) Hill, G. S.; Irwin, M. J.; Levy, C. J.; Rendina, L. M.; Puddephatt, R. J. *Inorg. Synth.* **1998**, *32*, 149−153.

mL of **2(TFE)** in TFE-d_3 by cooling with an ice or dry ice bath. The NMR spectra of these solutions show a new set of signals corresponding to **2(DME)**: ^{1}H NMR (600 MHz, TFE-d_6) δ = 0.85 (s, 3H), 1.37 (s, 9H), 1.38 (s, 9H), 1.89 (s, 3H), 1.99 (s, 3H), 6.84 (s, 2H), 7.04 (s, 2H), 7.54 (s, 1H), 7.54 (s, 1H); the equilibrium constant relating the two solvated complexes was determined from the relative peak intensities as a function of [DME]. At 313 K, signals for **2** gradually disappeared and were replaced by a new set of signals corresponding to **5**, which in turn decreased as crystals of **5** began to precipitate. Formation of **5** (by NMR) is nearly quantitative; isolated yields of crystalline **5** are generally 50% or less, depending on concentrations.

Kinetics of Dimethyl Ether Activation. Solutions of **2(TFE)** and DME in J. Young NMR tubes were prepared as described in the preceding section. After allowing to warm to room temperature and mixing, the sample height was measured to ±0.5 mm and compared with the starting height to correct the concentration of **2(TFE)** for the change in volume due to the dissolved gas. The concentration of added DME was determined by NMR, by comparing the integral of free DME with the integral of **2**. Tubes were inserted in the NMR spectrometer that had been preheated to 313 ± 0.5 K, and kinetics were monitored by following the disappearance of the starting material in the ^{1}H NMR spectrum.

[(Diimine)Pt(μ-CH_2)(μ-(CH(OCH_3))Pt(diimine)]$^{2+}$[$CF_3CD_2OB(C_6F_5)_3]^-_2$ (5). Crystals that precipitated at the end of dimethyl ether activations were isolated by filtration and dried under vacuum. These crystals were very soluble in organic solvents, including diethyl ether. Removing the solvent from these solutions gave oily residues rather than solids. Redissolving the crystals in acetone-d_6 gave a sample that is 90% **5**. ^{1}H NMR (500 MHz, acetone-d_6): δ = 1.278 (s, 9H), 1.283 (s, 9H), 1.29 (s, 9H), 1.30 (s, 9H), 2.25 (s, 3H), 2.26 (s, 3H), 3.79 (s, 3H), 6.78 (at, J_{H-H} = 1.8 Hz, 1H), 6.83 (at, J_{H-H} = 1.8 Hz, 1H), 6.91 (at, J_{H-H} = 1.8 Hz, 1H), 6.93 (at, J_{H-H} = 1.8 Hz, 1H), 7.46 (m, 2H), 8.01 (d, J_{H-H} = 5.25 Hz, 1H), 8.15 (dd, J_{H-H} = 5.25 Hz, J_{H-H} = 1.74 Hz, 1H), 10.35 (d, J_{H-H} = 1.74 Hz, 1H); HRMS (FAB) *m*/*z* calcd for $[C_{67}H_{102}N_4OPt_2]^+$ 1368.735, found 1368.733.

X-ray Structure of 5. A crystal obtained as described above was analyzed. Best results were obtained by refining the structure in space group $P\bar{1}$, wherein the Pt dimer sits on a center of symmetry, with the μ-CH_2 and μ-CH(OCH_3) groups disordered with respect to this center of symmetry; the methoxy group occupies each of the two sites with equal probability. Attempts to solve the structure in *P*1 gave less reliable results. Full details of the solution and refinement are available.[14]

Acknowledgment. We thank Michael Day and Larry Henling for assistance with X-ray crystallography, and Dan Nieman, Dean Roddick, Steve Olson, Mike Roy, David Law, Glenn Sunley, and Marc Payne for assistance with design and construction of the high-pressure NMR equipment. We are grateful to bp for financial support through the MC^2 program.

Supporting Information Available: Complete author list for ref 1. This material is available free of charge via the Internet at http://pubs.acs.org.

JA056387T